Ultrahigh spatiotemporal Resolution Beam Signal Reconstruction with bunch phase compensation

Youming Deng,[1,2,3] Yongbin Leng,[4,1,2,*] Xingyi Xu,[1,2,3] Jian Chen,[5,3] and Zhou Yimei[5,3]

[1]*Shanghai Institute of Applied Physics, Chinese Academy of Sciences, Shanghai 201800, China*
[2]*University of the Chinese Academy of Sciences, Beijing 100049, China*
[3]*Shanghai Synchrotron Radiation Facility, Chinese Academy of Sciences, Shanghai 201204, China*
[4]*University of Science and Technology of China, Hefei 230026, China*
[5]*Shanghai Advanced Research Institute, Chinese Academy of Sciences, Shanghai 201204, China*

Various electromagnetic signals are excited by the beam in the acceleration and beam-diagnostic elements of a particle accelerator. It is important to obtain time-domain waveforms of these signals with high temporal resolution for research, such as the study of beam-cavity interactions and bunch-by-bunch parameter measurements. Therefore, a signal reconstruction algorithm with ultrahigh spatiotemporal resolution and bunch phase compensation based on equivalent sampling is proposed in this paper. Compared with traditional equivalent sampling, the use of phase compensation and setting the bunch signal zero-crossing point as the time reference can construct a more accurate reconstructed signal. The basic principles of the method, simulation, and experimental comparison are also introduced. Based on the beam test platform of the Shanghai Synchrotron Radiation Facility (SSRF) and the method of experimental verification, the factors that affect the reconstructed signal quality are analyzed and discussed, including the depth of the sampled data, quantization noise of analog-to-digital converter (ADC), beam transverse oscillation, and longitudinal oscillation. The results of the beam experiments show that under the user operation conditions of the Shanghai Synchrotron Radiation Facility (SSRF), a beam excitation signal with an amplitude uncertainty of 2% can be reconstructed.

Keywords: turn-by-turn bunch phase compensation technique; equivalent sampling; signal reconstruction algorithm; ultrahigh spatio-temporal resolution; SSRF.

I. INTRODUCTION

Many electromagnetic signals are excited by electron beams in beam pipes, accelerators, and the beam diagnostic elements of particle accelerators [1, 2]. These signals usually consist of a mixture of various oscillating modes and change rapidly with time [3, 4]. Therefore, obtaining the time domain waveforms of these signals with high temporal resolution is important for the study of related problems, such as the beam-cavity interaction and the measurement of bunch-by-bunch beam parameters.

These types of signals can be calculated using analytical or numerical simulation methods [5–8]. However, it is difficult to complete the calculation when the structure of the beam vacuum chamber is complex, and it is difficult to judge whether the calculation results are sufficiently accurate. Therefore, it is necessary to explore experimental methods for measuring such signals with high temporal resolution. In addition, high-precision bunch-by-bunch measurements have become a focus of accelerator research worldwide in recent years owing to the advancement of electronic technology and the requirement for accelerator machine research [9–19].

However, the time resolution (sampling rate) and voltage resolution (effective number of bits) of the actual sampling equipment are constrained by various conditions [20]. In beam measurement, the excitation signal of the electrode is often very narrow in the time domain. Taking the Shanghai Synchrotron Radiation Facility (SSRF) as an example, the pulse signal of a single-bunch excitation has a width of less than 500 ps in the time domain, and the wakefield signal has a width of hundreds of ps [21]. In addition, the amplitude of the wakefield signal is relatively small compared to the bunch signal, which requires a larger voltage resolution to measure it effectively [22, 23]. Therefore, there is a high demand for both time resolution and voltage resolution. While conducting this research at the beam instrumentation (BI) Group of the Shanghai Synchrotron Radiation Facility (SSRF), we could not find any sampling equipment that met market requirements.

A set of technologies for 3D bunch-by-bunch position measurements based on a high-sampling-rate oscilloscope was recently developed by the Beam Instrumentation (BI) Group of the Shanghai Synchrotron Radiation Facility (SSRF) [24, 25]. The core algorithm of this technology is the response function projection method of the electrode to bunch signal. To obtain ultrahigh time resolution and ultrahigh voltage resolution response functions based on the equivalent sampling principle and statistical method, a data processing technique was developed to reconstruct the high-resolution periodic beam signal using the measured data.

This paper provides a comprehensive introduction to the basic principles, simulations, and an experimental comparison of this method. By conducting beam experiments, the relationships between the quality of the reconstructed signal and the sampling rate of the data acquisition equipment, the depth of the sampled data, and the quantization noise of the ADC were analyzed. Additionally, the quality of the reconstructed signal under different beam conditions was investigated, and the impact of transverse and longitudinal beam position changes on signal reconstruction was discussed.

* Corresponding author, Yongbin Leng, lengyb@ustc.edu.cn.

II. BASIC PRINCIPLE

A. Equivalent Sampling

To better match the measurement of various parameters in the beam measurement, the extraction of the zero-crossing point of the pulse signal was used as the time zero point for the coordinate axis in this study, instead of using the starting sampling point, as in traditional equivalent sampling [26]. Moreover, this zero point is used to characterize the phase zero point of the beam bunch.

We assume that the excitation signal of the beam bunch is sufficiently stable and can be considered as a periodic signal with a revolution period within a certain time interval. When an ideal data acquisition system is used to digitize the bunch signal $s(t)$ with $2N+1$ sampling samples, the result of the n th sampling can be expressed as

$$x(n) = s(T_0 + nT_s). \tag{1}$$

where $n = -N, -(N-1), ..., -1, 0, 1, 2...N$, T_0 is the zero-crossing point of the pulse signal, and T_s is the sampling period.

Because the signal is considered periodic, it can be expressed as

$$s(t) = s(t + kT). \tag{2}$$

where $k = 0, 1, 2, 3, ..., T$ is the period of the signal.

The same signal is sampled several times by adjusting the initial sampling time. For example, by adjusting the initial sampling time step to Δt and the sampling time to M, the sampling result can be expressed as

$$x(n, m) = s(T_0 + m\Delta t + nT_s). \tag{3}$$

where $n = -N, -(N-1), ..., -1, 0, 1, 2...N, m = 1, 2, 3...M$.

If the results of multiple samplings are equivalent to the same signal period, the sampling rate can be increased. The sampling rate is known as the equivalent rate. Theoretically, if there is an integer multiple relationship between T_s and Δt, the equivalent sampling time interval can be reduced to Δt, which corresponds to the equivalent sampling rate increasing from $1/T_s$ to $1/\Delta t$ [27, 28].

Figure 1 (a) shows a typical waveform of the equivalent sampled using the dashed blue line. It exhibits a signal with a period of 2000 ps. To sample the waveform three times using an ideal ADC, 12 points were sampled for each period. Based on the principle of equivalent sampling, mapping the data collected from the three cycles onto a single cycle can result in a higher relative sampling rate for the sampled signal, as shown in Fig. 1 (b). However, the bunch signal was not strictly periodic. The waveform represented by the dashed red line in Fig. 1 (a) represents the sampling of a bunch signal with longitudinal oscillations. If the waveform is directly reconstructed based on the traditional equivalent sampling method, the results are as shown in Fig. 1 (c). The blue circles represent the equivalent sampling points and the dashed red line represents the original signal waveform. It can be observed from the Fig. 1 (c) that the sampling points have deviated significantly from the true values. Furthermore, Fig. 1 (d) represents the reconstruction result after applying the turn-by-turn bunch phase compensation technique. The use of the turn-by-turn bunch-phase compensation leads to a reconstructed signal that closely matches the source signal.

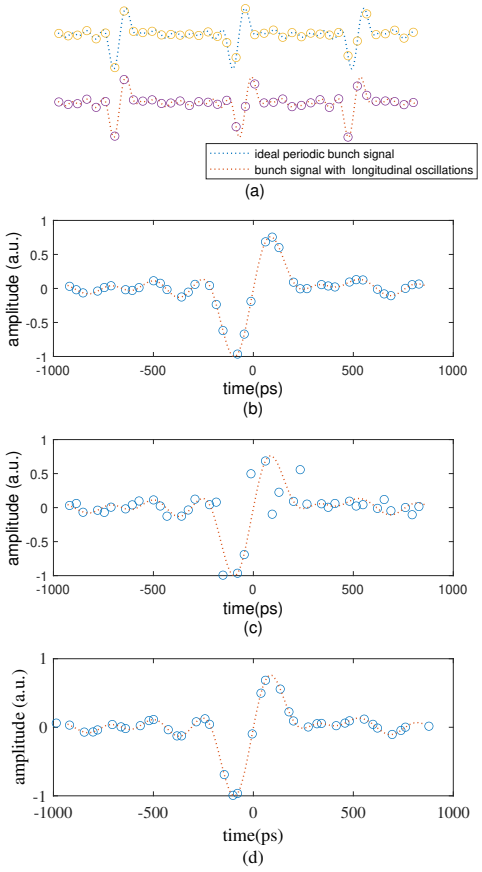

Fig. 1. (a) Diagram of equivalent sampling (b) Traditional equivalent sampling. (c) Traditional equivalent sampling with longitudinal oscillations. (d) Equivalent sampling reconstruction with turn-by-turn bunch phase compensation technique.

B. Signal Reconstruction

For ideal periodic signals and ADCs, the reconstructed signals should exhibit smooth curves. However, actual bunch signals are not strictly periodic. It exhibited certain longitudinal and transverse oscillations, and the ADC exhibited quantization errors and time jitter. To reduce the error caused by beam oscillations, the voltage and time of each sampling (data

for each ring of the beam) were subtracted from the calculated transverse and longitudinal oscillations to approximate the real bunch waveform. To reduce the random error introduced by the ADC, the reconstructed signal was sliced by time, and the most probable value in each slice was used to represent the value, with the time midpoint used to represent the time.

As shown in Fig. 2 (a), for a signal with a period of 2000 ps, if an ADC with a time interval of 100 ps (sampling rate of 10 GHz) is used for digitalization, 7000 samplings are performed, with 20 sample points each time and a 3 ps earlier starting time for each sampling. After splitting 7000 sets of sampling data, a set of reconstructed data with an equivalent sampling rate of 70THz was obtained. The blue waveform represents the reconstructed signal before subtracting the oscillation, and the orange waveform represents the reconstructed signal after subtracting the oscillation. In this case, the beam oscillation was relatively small, and no significant difference was observed, as shown in Fig. 2 (a). In the subsequent analysis, the impact of the beam oscillation on the quality of the reconstructed signal was further discussed and experimentally verified.

The reconstructed signal was divided into 100 time slices, with the midpoint representing the time of each slice. Figure 2 (c), (d), (e), and (f) show the frequency distribution histograms of slices 21st, 41st, 61st, and 81st slices, respectively. The curves in the figures represent normal distribution fitting curves. The value corresponding to the maximum frequency was considered the value for each slice. Thus, the response function is obtained via spline interpolation as shown in Fig. 2 (b).

According to the principle of the equivalent sampling and signal reconstruction method, the sampled signal should satisfy the following conditions: it should be periodic (strictly repetitive) or quasi-periodic (with negligible variation during sampling) and have a high signal-to-noise ratio.

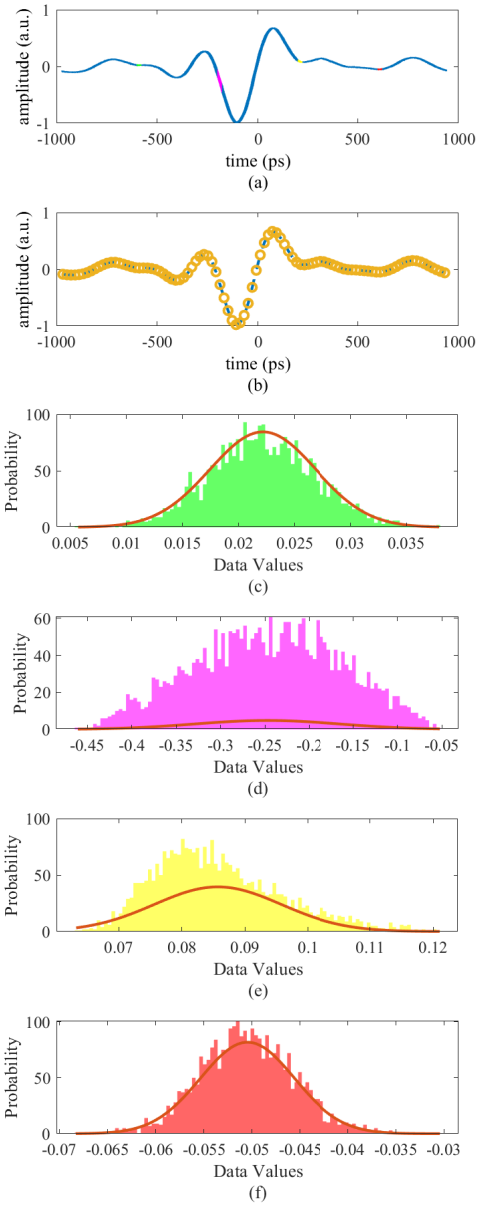

Fig. 2. (a) Reconstructed signal of equivalent sampling. (b) Reconstructed signal waveform after spline interpolation. (c) Frequency distribution histograms of the 21st slice. (d)Frequency distribution histograms of the 41st slice. (e) Frequency distribution histograms of the 61st slice. (f) Frequency distribution histograms of the 81st slice.

III. UNCERTAINTY ANALYSIS

In the actual sampling process, the beam signal is not strictly periodic and contains nonrandom disturbances, such as longitudinal oscillations. These processes are deterministic and measurable and can be considered during signal reconstruction to refine the beam signal and make it closer to a periodic signal. Additionally, for a non-ideal ADC, the sampled data contain random noise, which can lead to excessive errors in the curve fitting or interpolation results.

A. Quantizing Noise

During the sampling process, the quantization noise can be approximated to follow a uniform distribution. If the quantization step size was δ, the quantization noise interval was $[-\delta/2, +\delta/2]$ [29, 30]. Therefore, the quantization noise can be expressed as:

$$n_q(t) \sim U(-\delta/2, +\delta/2). \tag{4}$$

where $n_q(t)$ is the quantization noise of the sampling point at time t and $U(-\delta/2, +\delta/2)$ represents a uniform distribu-

tion over the interval $[-\delta/2, +\delta/2]$.

Because the quantization noise is additive, when only quantization noise is considered, the sampled signal can be expressed as

$$x(t) = s(t) + n_q(t). \tag{5}$$

where $x(t)$ is the sampled signal, $s(t)$ is the real signal, and $n_q(t)$ is quantization noise.

Therefore, at any time t_0, the sampled signal satisfies

$$x(t_0) \sim U(s(t_0) - \delta/2, s(t_0) + \delta/2). \tag{6}$$

Therefore, for time t_0, the sampled signal of this point satisfies the probability density distribution, whose mean value is the most probable value of this point.

Based on the above analysis, a quantization noise with 2% of the original signal amplitude as δ was constructed for the simulation. The most probable value for each point was considered the result of the reconstructed signal. The relative uncertainty of the reconstructed signal was obtained via point-by-point subtraction of the original and reconstructed signals. The results show that when only quantization noise is present in the system, the uncertainty of the reconstructed signal is randomly distributed over the entire time domain and the relative uncertainty of the reconstructed signal is less than 1×10^{-2} for the quantization noise with δ, which is 2% of the signal amplitude.

B. Time Jitter

Similar to quantization noise, time jitter is a random signal at the sampling time and follows a normal distribution with expectation zero and variance σ_t, which is negatively related to the clock stability of the ADC [31]. Therefore, for any sampling point, the sampling time t_0 meets:

$$t_0 \sim N(t_0, \sigma_t). \tag{7}$$

Assuming that the sampling time t_0 and real signal s satisfy the mapping relation f, the probability distribution of the sampled signal at time t_0 is shown in Fig. 3 (a). According to the probability distribution of the sampled signal, it can be inferred that when the real signal satisfies monotonicity near the sampled point, the sampled signal follows a quasi-normal distribution, with the real value of the point as the most probable value, and the mapping relation f affects the sparsity of the probability density on both sides of the most probable value. When the real signal has an extreme point near the sampling point, if there is $f(t_1) = f(t_2)$ such that $p(t_1)+p(t_2) > p(t_0)$, where p represents the probability density at the corresponding time, then the most probable value is not equal to the value of the real signal at this point. Otherwise, the most likely value of this point is the value of the real signal at this point.

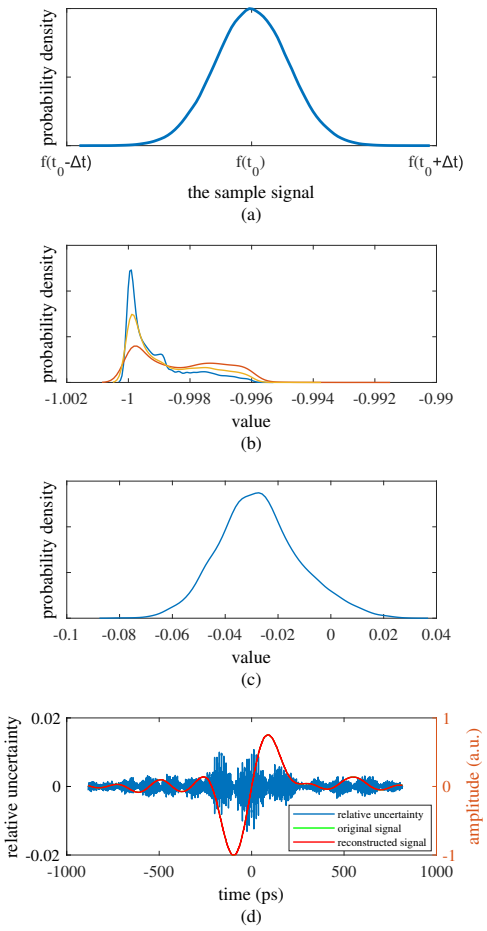

Fig. 3. (a) Probability density distribution of the sampled signal with time jitter. (b) Probability density distribution around the negative peak. (c) Probability density distribution away from the peak. (d) Relative uncertainty of the reconstructed signal.

Based on the above analysis, the clock jitter with a variance of 1 ps (the period of the original signal was 2000 ps, and the time interval was 0.1ps.) and mean of 0, constructed. The sample number for each point was 10000, and the frequency distribution at each point was calculated. Figures 3 (b), (c) show the results. As shown in Fig. 3 (b) and (c), the simulation results are similar to those of the uncertainty analysis. At points away from the peak, the sample distribution followed an approximately normal distribution, and the most probable value was approximately the true value. Near the peak point, the frequency distribution of the sample no longer followed a normal distribution; however, the most probable value approximated the value of the peak point. Therefore, the most probable value can also be used to characterize the true value of a point.

The most probable value for each point was considered the result of the reconstructed signal. The relative uncertainty of

the signal reconstructed by the proposed method can be obtained by subtracting the reconstructed signal from the most probable distribution of the original signal, as shown in Fig. 3 (d). In addition, Fig. 3 (d) shows that the effect of time jitter on the signal reconstruction is mainly concentrated away from the peak, and the uncertainty is small near the peak. For a beam signal with a period of 2000 ps and a time interval of 0.1 ps, the relative uncertainty caused by the time jitter is less than 1×10^{-2}.

The existing acquisition equipment in our laboratory belongs to Keysight's Infiniium MXR series, with a clock jitter of approximately 120 fs, which is far less than the ps-level beam longitudinal oscillation during the user operation conditions of the Shanghai Synchrotron Radiation Facility (SSRF). Therefore, in the actual experiments, the error in the time dimension mainly originates from the beam's longitudinal oscillation, and the influence of the clock jitter on this method can be neglected.

IV. EVALUATION METHOD

This paper proposes methods for evaluating the quality of reconstructed signals under different conditions. One method involves calculating the standard deviation between the reconstructed and reference signals, which requires a relatively clear reference signal that may not exist in practical experiments. Therefore, the best measurement result obtained under the optimal experimental conditions was selected as the reference signal to evaluate the relative uncertainty.

Another method involves evaluating the local quality of the reconstructed signal by calculating the second-order difference in the signal, which indicates the degree of signal unsmoothness. The standard deviation of the second-order difference of the reconstructed signal was calculated to evaluate the overall quality of the reconstructed signal, which is referred to as relative noise in this study.

V. BEAM EXPERIMENT

The Shanghai Synchrotron Radiation Facility (SSRF) is a third-generation synchrotron radiation source with an electron energy of 3.5 GeV, featuring high current intensity, high brightness, high beam stability, and low emittance. For the storage ring of the SSRF, the RF frequency was 499.654 MHz, and the harmonic number was 720 [32]. Based on the above parameters, to analyze the relationship between different acquisition system parameters, different beam conditions, and the quality of the reconstructed signal, a series of beam experiments are designed accordingly for verification.

A. The SNR of Sampled Data

When the SSRF operates under the user operation conditions, the filling mode of the bunch in the storage ring is shown in Fig. 4 (a). There are 720 buckets in total filled with 500 bunches, each of which is divided into four bunch trains, each containing 125 bunches, with 55 buckets spaced. Each bunch train is nearly uniformly distributed; however, there are bunches with larger or smaller charges at the head and tail of each bunch train. The range is fixed during a single sampling event using an oscilloscope, resulting in different signal-to-noise ratios (SNRs) between bunches with varying charges. Therefore, we evaluated the impact of SNR on the quality of the response function by comparing the responses of bunches with different charges based on single-sampling data collected by the oscilloscope.

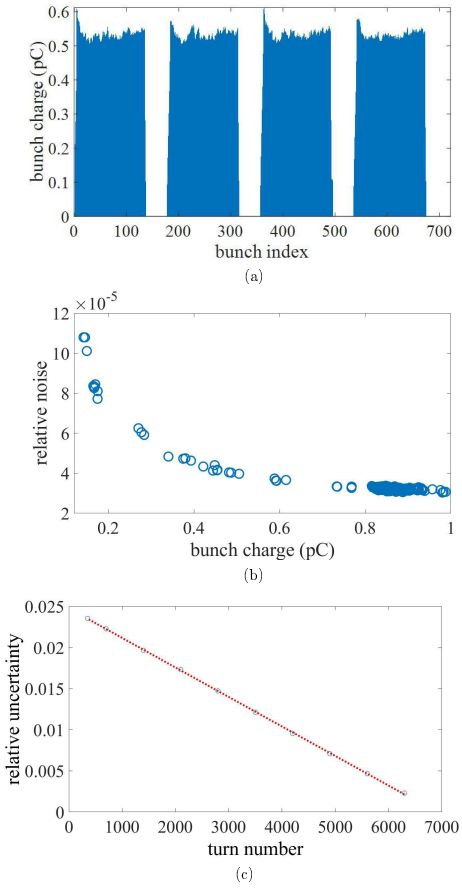

Fig. 4. (a) Filling pattern. (b) Quality of the reconstructed signal with different charges. (c) Relative uncertainty of the reconstructed signal with different depths of sampled data.

The response functions were constructed separately for bunches with different charges, and the second-order differences of the response functions were then calculated. The standard deviation of the second-order difference over the entire period gives the result shown in Fig. 4 (b), where it can be seen that there is an approximately inverse relationship between the bunch charge and the relative noise for the range of 0.1pc to 1pc. Therefore, the SNR of the sampled signal and the quality of the reconstructed signal were approximately inversely proportional within the experimental measurement range.

B. The Depth of Sampled Data

In this experiment, the effects of different sampling depths were evaluated equivalently by truncating the data for different lengths of the same sampling, where the data length was measured in the number of beam turns. From a statistical perspective, the larger the sample size, the higher the expected statistical results. Therefore, in this experiment, the maximum depth of the oscilloscope was approximately 7000 turns selected as the benchmark for calculating the relative uncertainty of different sampling depths. The results are presented in Fig. 4 (c). It can be observed that the greater the number of sampling groups, the smaller the relative uncertainty and the better the signal reconstruction quality.

C. Beam Transverse Oscillation

To assess the impact of beam transverse oscillation on the quality of the reconstructed signal, the transient process during storage-ring injection was used as a suitable window because it exhibits strong transverse oscillation. Therefore, the experimental data selected for analysis contained the storage ring injection. As shown in Fig. 5 (a), these data are injected after approximately 800 turns, resulting in a transverse oscillation of approximately $\pm$1mm. Figure 5 (b) shows the normalized amplitudes of the signal peak values obtained by a single electrode for the same bunch at different turns, which were used to characterize the beam transverse oscillation. As shown in Fig. 5 (b), there was a relative change of 10% after the injection.

Signals were reconstructed using data from the first 800 turns during injection. The first 800 turns were not affected by the beam injection; therefore, they were used as benchmarks. The relative uncertainty was obtained by subtracting the two reconstructed signals, as shown in Fig. 5 (c). From these results, it can be speculated that the relative uncertainty of the reconstructed signal can reach approximately 2% when there is a 10% transverse oscillation in the beam signal. Therefore, under the condition of transverse oscillation, if the required accuracy of the constructed signal is less than 2%, the influence of transverse oscillation can be ignored, and the signal can be directly constructed; however, when the required accuracy is better than 2%, the data with small transverse oscillation or the refined method should be selected to construct the reconstructed signal.

D. Beam Longitudinal Oscillation

To analyze the influence of longitudinal oscillations on the quality of the reconstructed signal, beam signals containing longitudinal oscillations were selected for evaluation, as shown in Fig. 6 (a). The longitudinal oscillation ranges from -6 to 2 ps.

Based on the actual longitudinal oscillation, the original data were refined by subtracting the bunch phase caused by the longitudinal oscillation per turn, and the reconstructed

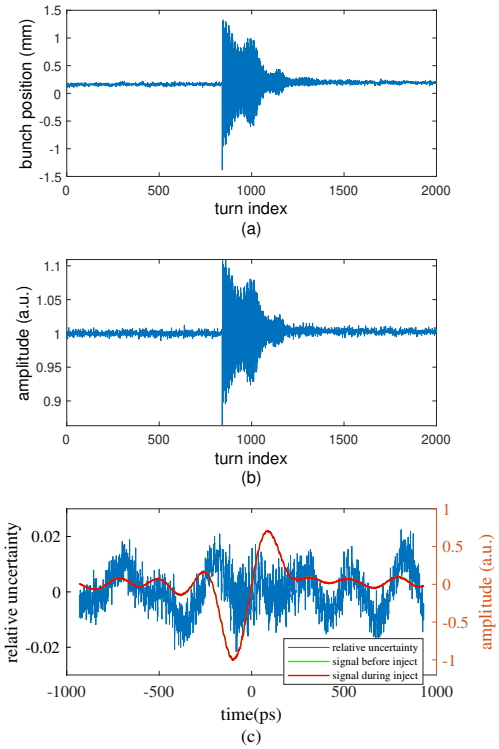

Fig. 5. (a) Transverse position of different turns. (b) Amplitude of the signal of different turns. (c) Relative uncertainty induced by transverse oscillation.

signal was constructed based on equivalent sampling. The difference between the refined results and the results of direct signal reconstruction without compensation is the relative uncertainty, as shown in Fig. 6 (b). As the reconstructed signal was normalized, the result in Fig. 6 (b) can also be viewed as the relative uncertainty from the longitudinal oscillation, with the relative uncertainty being better than 2×10^{-3}.

Furthermore, the second-order difference in the reconstructed signal before and after compensation can be calculated as relative noise, as shown in Fig. 6 (c) and (d). Compared with the reconstructed signal, it can be seen that the relative noise is larger at the point with a larger slope of the reconstructed signal, and this part of the difference can be significantly reduced by refining the original data.

In addition, the storage ring may be in different longitudinal oscillation states according to the machine conditions, and another set of data with different oscillation states was selected for the experimental analysis. As shown in Fig. 6 (e), the longitudinal oscillations range from a few ps to -300 ps. Similarly, the results in Fig. 6 (f) can be obtained by reconstructing the original signals before and after compensation and then taking the difference as the relative uncertainty. Clearly, when the amplitude of the longitudinal oscillation is large, the uncertainty is very large, and the relative uncertainty reaches 10% under the conditions of this experiment.

In summary, for the different acquisition systems, the

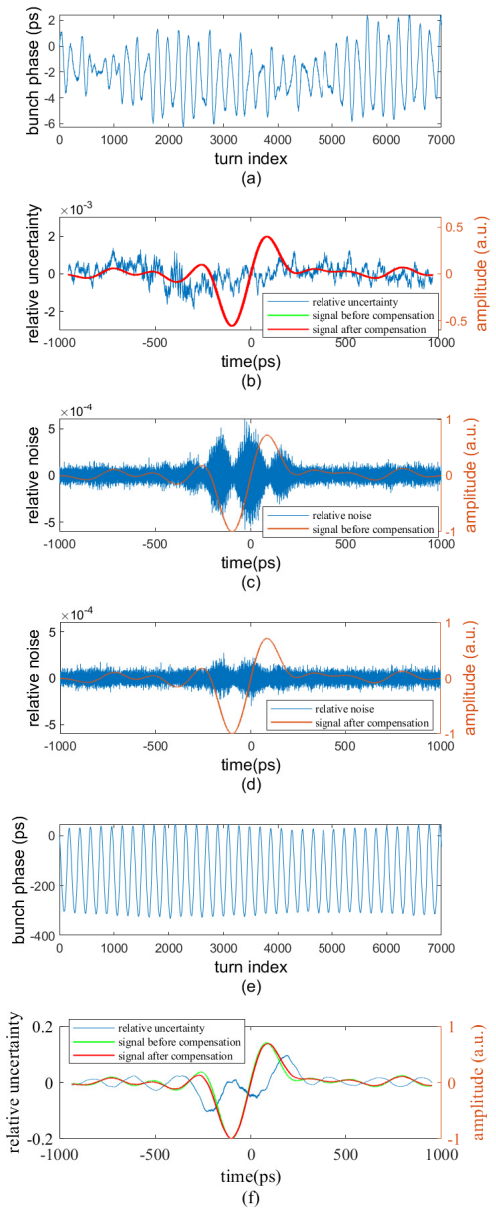

Fig. 6. (a) Variation diagram of longitudinal oscillation. (b) Relative uncertainty from longitudinal oscillation. (c) Relative noise of the reconstruction signal before compensation. (d) Relative noise of the reconstruction signal after compensation. (e) Variation diagram of the larger longitudinal oscillation. (f) Relative signal difference between amplitude before and after compensation

higher the number of ADC sampling bits and the larger the sampling depth, the better the quality of the reconstructed signal. For different beam conditions, longitudinal oscillations with large amplitudes must be compensated before signal reconstruction; otherwise, the authenticity of the reconstructed signal cannot be guaranteed. However, for transverse and small longitudinal oscillations, compensation can be selected according to the system requirements.

VI. PERFORMANCE EVALUATION

Based on the beam experiment, 200 sets of beam data at different times with a maximum sampling depth (7000 turns), maximum sampling signal-to-noise ratio, and negligible transverse and longitudinal oscillations were selected for signal reconstruction. The standard deviations of 200 sets of reconstructed signals were calculated point-by-point after normalization. The relative amplitude uncertainty was characterized by this standard deviation, as shown in Fig. 7. Therefore, for the signal reconstruction method proposed in this study, the relative amplitude uncertainty is better than 2% when the sampling depth is at its maximum, the sampling signal-to-noise ratio is at its maximum, and the lateral and longitudinal oscillations are negligible.

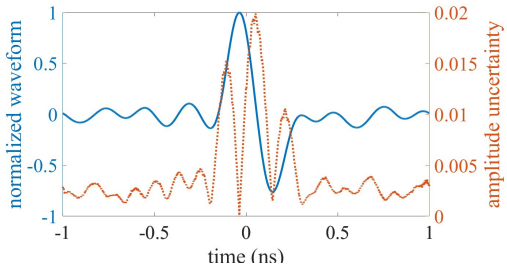

Fig. 7. Relative uncertainty of reconstructed signal at different times.

VII. CONCLUSION

A reconstruction method for periodic beam signals in an electron storage ring was developed based on the principle of equivalent sampling. Compared with traditional equivalent sampling, when constructing the reconstructed signals of each bunch, the effect of multiturn bunch instability is reduced by subtracting the transverse and longitudinal oscillations. The zero-crossing point of the signal pulse is taken as the time zero point, which is conducive to the subsequent study of signals, such as the wakefield of the beam based on the bunch.

Beam excitation signals with a relative amplitude uncertainty of 2% could fully satisfy the requirements of the response function of the bunch-by-bunch 3D measurement system. The reconstructed signal bandwidth in this paper was 4.2 GHz, and this method has no bandwidth limitations. If the data acquisition equipment and signal transmission networks are upgraded, they can be used to process signals with higher bandwidths. Therefore, this method can be extended to the sampling analysis of wakefield signals with bandwidths of tens of GHz bandwidth.

[1] X.Y. Xu, Y.B. Leng, Y.M. Zhou et al., Bunch-by-bunch three-dimensional position and charge measurement in a storage ring. Phys. Rev. Accel. Beams. **24**, 032802 (2021). doi: 10.1103/PhysRevAccelBeams.24.032802

[2] J.J. Liu, X.P. Ma, G.X. Pei et al., Phase-stabilized RF transmission system based on LLRF controller and optical delay line. Nucl. Sci. Tech. **30**, 177 (2019). doi: 10.1007/s41365-019-0697-9

[3] C. Wang, J.H. Tan, X.X. Huang et al., Design optimization and cold RF test of a 2.6-cell cryogenic RF gun. Nucl. Sci. Tech. **32**, 97 (2021). doi: 10.1007/s41365-021-00925-8

[4] S.C. Jiang, G. Xu, Examining RF jitter and transverse mode-coupling instability in triple-frequency RF systems. Nucl. Sci. Tech. **31**, 45 (2020). doi: 10.1007/s41365-020-00752-3

[5] A. Angelovski, A. Kuhl, M. Hansli et al., High bandwidth pickup design for bunch arrival-time monitors for free-electron laser. Phys. Rev. ST Accel. Beams. **15**, 1120803 (2012). doi: 10.1103/PhysRevSTAB.15.112803

[6] L. Wang, J.C. Yang, M.X. Chang et al., GOAT: a simulation code for high-intensity beams. Nucl. Sci. Tech. **34**, 78 (2023). doi: 10.1007/s41365-023-01225-z

[7] G. Franchetti, Space charge in circular machines. CERN-2017-006-SP, p. 353. doi: 10.23730/CYRSP-2017-003

[8] M.H. Song, C. Feng, D.Z. Huang et al., Wakefields studies for the SXFEL user facility. Nucl. Sci. Tech. **28**, 90 (2017). doi: 10.1007/s41365-017-0242-7

[9] H.J. Chen, J. Chen, B. Gao et al., Bunch-by-bunch beam size measurement during injection at Shanghai Synchrotron Radiation Facility. Nucl. Sci. Tech. **29**, 79 (2018). doi: 10.1007/s41365-018-0420-2

[10] Z.J. Qiu, K. Li, H.L. Xie et al., Study of 20 Hz high spatial-temporal resolution monochromatic X-ray dynamic micro-CT. NUCLEAR TECHNIQUES **46**, 070101 (2023). doi: 10.11889/j.0253-3219.2023.hjs.46.070101.

[11] G. Kotzian, Transverse Feedback Parameter Extraction from Excitation Data. in Proc. 8th Int. Particle Accelerator Conf. (IPAC'17), Copenhagen, Denmark, May 2017, paper TUPIK094, pp. 1920-1923, ISBN: 978-3-95450-182-3. doi: 10.18429/JACoW-IPAC2017-TUPIK094

[12] Y.G. W, T. Zhang, Z.Z. X et al., Real Time Bunch-by-Bunch Luminosity Monitor for BEPCII. 2008 IEEE Instrumentation and Measurement Technology Conference, Victoria, BC, Canada, 2008, pp. 1155-1158. doi: 10.1109/IMTC.2008.4547213

[13] R. Farias, L. Liu, A. Rodrigues et al., Oscilloscope measurement of the synchronous phase shift in an electron storage ring. Phys. Rev. ST Accel. Beams. **4**, 072801 (2001).doi:10.1103/PhysRevSTAB.4.072801

[14] T. Ieiri, K. Akai, H. Fukuma et al., Bunch-by-bunch measurements of the betatron tune and the synchronous phase and their applications to beam dynamics at KEKB. Phys. Rev. ST Accel. Beams. **5**, 094402 (2002). doi: 10.1103/PhysRevSTAB.5.094402

[15] Z.C. Chen, Y. Yang, Y.B. Leng et al., Wakefield measurement using principal component analysis on bunch-by-bunch information during transient state of injection in a storage ring. Phys. Rev. ST Accel. Beams. **17**, 112803 (2014).doi: 10.1103/PhysRevSTAB.17.112803

[16] Y.M. Zhou, H.J. Chen, S.S. Cao et al., Bunch-by-bunch longitudinal phase monitor at SSRF. Nucl. Sci. Tech. **29**, 113 (2018). doi: 10.1007/s41365-018-0445-6

[17] X.Y. Xu, Y.M. Zhou, Y.B. Leng, Machine learning based image processing technology application in bunch longitudinal phase information extraction. Phys. Rev. Accel. Beams. **23**, 032805 (2020).doi: 10.1103/PhysRevAccelBeams.23.032805

[18] D.R. Bett, N.B. Kraljevic, T. Bromwich et al., High-resolution, low-latency, bunch-by-bunch feedback system for nanobeam stabilization. Phys. Rev. Accel. Beams. **25**, 022801 (2022). doi: 10.1103/PhysRevAccelBeams.25.022801

[19] J.L. Steinmann, T. Boltz, M. Brosi et al., Continuous bunch-by-bunch spectroscopic investigation of the microbunching instability. Phys. Rev. Accel. Beams. **21**, 110705 (2018). doi: 10.1103/PhysRevAccelBeams.21.110705

[20] Z. Zhou, S.G. Li, Q.S. Tan et al., Optimization method of Hadamard coding plate in γ-ray computational ghost imaging. Nucl. Sci. Tech. **34**, 13 (2023). doi: 10.1007/s41365-022-01164-1

[21] Y. Yang, Y.B. Leng, Y.B. Yan et al., Development of the bunch-by-bunch beam position acquisition system based on BEEcube. Nucl. Sci. Tech. **27**, 47 (2016). doi: 10.1007/s41365-016-0035-4

[22] W. Liu, D.S. Doran, G. Ha et al., LLRF Upgrade at the Argonne Wakefield Accelerator Test Facility. in Proc. IPAC'21, Campinas, SP, Brazil, May 2021, pp. 2176-2177. doi: 10.18429/JACoW-IPAC2021-TUPAB296

[23] J. Upadhyay, E.I. Simakov et al., Simulations and Measurements of the Wakefield Loading Effect in Argonne Wakefield Accelerator Beamline. in Proc. 9th Int. Particle Accelerator Conf. (IPAC'18), Vancouver, BC, Canada, Apr. 4,, pp. 4675-4677. doi: 10.18429/JACoW-IPAC2018-THPML012

[24] X.Y. Xu, Y.B. Leng, Y.M. Zhou et al., New noninvasive measurement method of optics parameters in a storage ring using bunch-by-bunch 3D beam position measurement data. Phys. Rev. Accel. Beams. **24**, 062802 (2021).doi: 10.1103/PhysRevAccelBeams.24.062802

[25] X.Y. Xu, Y.B. Leng, B. Gao et al., HOTCAP: a new software package for high-speed oscilloscope-based three-dimensional bunch charge and position measurement. Nucl. Sci. Tech. **32**, 131 (2021). doi: 10.1007/s41365-021-00966-z

[26] H.C. Dong, L.L. Pang, S. Li et al., Monitoring System of Debris Flow Water Level Based on Equivalent Sampling Method. In: Chang, JW., Yen, N., Hung, J.C. (eds) Frontier Computing. FC 2020. Lunk Notes in Electrical Engineering, vol 747. Springer, Singapore. doi: 10.1007/978-981-16-0115-6_191

[27] D. Lee, J. Sung and J. Park, A 16ps-resolution Random Equivalent Sampling circuit for TDR utilizing a Vernier time delay generation. IEEE Nuclear Science Symposium, 2003. A conference Record (IEEE Cat. No.03CH37515), Portland, OR, USA, 2003, pp. 1219-1223 Vol.2. doi: 10.1109/NSS-MIC.2003.1351912

[28] C. Chen, S. Wu, S. Meng et al., Application of Equivalent-Time Sampling Combined with Real-Time Sampling in UWB Through-Wall Imaging Radar. 2011 First International Conference on Instrumentation, Measurement, Computer, Communication and Control, Beijing, China, 2011, pp. 721-724. doi: 10.1109/IMCCC.2011.183

[29] R.M. Gray, Quantization noise spectra. IEEE Trans. Inf. Theor. **36**, 1220–1244 (1990). doi: 10.1109/18.59924

[30] A.N. Serov, D.A. Chumachenko and A.A. Shatokhin, Application of Random Functions to Assess the Influence of Quantization Error on the Signal RMS. 2020 Ural Smart Energy Conference (USEC), Ekaterinburg, Russia, 2020, pp. 43-46. doi:

10.1109/USEC50097.2020.9281188

[31] Yamaguchi, T.J., Ishida, M., Soma, M. et al. Timing-jitter measurement of intrinsic random and sinusoidal jitter using frequency division. Journal of Electronic Testing **19**, 183–193 (2003). doi: 10.1023/A:1022897825759

[32] W.H. Wu, L. Zhao, E. Chen et al., Optimization of the sampling process for the close orbit data in the digital Beam Position Measurement for SSRF. 2014 IEEE Nuclear Science Symposium and Medical Imaging Conference (NSS/MIC), Seattle, WA, 2014, pp. 1-3. doi: 10.1109/NSSMIC.2014.7431102